

# Magnetic moment of a single metal nanoparticle determined from the Faraday effect

Jacek Szczytko,<sup>1,\*</sup> Nataša Vaupotič,<sup>2,3</sup> Karolina Madrak,<sup>4</sup> Paweł Sznajder,<sup>1</sup> and Ewa Górecka<sup>4</sup>

<sup>1</sup>*Institute of Experimental Physics, Faculty of Physics, University of Warsaw, Hoza 69, 00-681 Warsaw, Poland*

<sup>2</sup>*Department of Physics, Faculty of Natural Sciences and Mathematics, University of Maribor, Koroška 160, 2000 Maribor, Slovenia*

<sup>3</sup>*Jozef Stefan Institute, Jamova 39, 1000 Ljubljana, Slovenia*

<sup>4</sup>*Department of Chemistry, University of Warsaw, Żwirki i Wigury 101, 02-089 Warsaw, Poland*

(Received 31 July 2012; revised manuscript received 12 November 2012; published 12 March 2013)

Optical properties of a composite material made of ferromagnetic metal nanoparticles embedded in a dielectric host are studied. We constructed an effective dielectric tensor of the composite material taking into account the orientational distribution of nanoparticle magnetic moments in external magnetic field. A nonlinear dependence of the optical rotation on magnetic field resulting from the reorientation of nanoparticles is demonstrated. The theoretical findings were applied to the magneto-optical experimental data of cobalt ferromagnetic nanoparticles embedded in a dielectric liquid host. The dependence of the Faraday rotation on Co-based ferromagnetic nanoparticles was measured as a function of the external magnetic field, varying the size of nanoparticles and the wavelength of light. The proposed approach enables quantitative determination of the magnetic moment and the plasma frequency of a single nanoparticle, and from this the size of the nonmagnetic shell of magnetic nanoparticles.

DOI: [10.1103/PhysRevE.87.033201](https://doi.org/10.1103/PhysRevE.87.033201)

PACS number(s): 41.20.-q, 75.75.-c, 78.20.Ls, 78.67.Sc

## I. INTRODUCTION

Compounds showing large magneto-optic effects are searched for because of their possible application in optical technology as fast shutters, switches, tunable phase retarders, etc. [1,2]. Magnetic materials are ideal for such applications, as due to the magnetic nature of compounds large optical linear and circular anisotropy can be induced by applying a relatively small external magnetic field. Among magnetic materials, a lot of attention was devoted to ferrofluids, i.e., solution of magnetic nanoparticles in nonmagnetic host, which are extensively studied experimentally since the 1970s; however, the origin of the magneto-optic effect in these materials is still not fully understood [3–9]. The most studied effect, the induced linear birefringence, has often been related to the shape anisotropy of nanoparticles or to the formation of anisotropic aggregates under magnetic field [10–17], while the optical activity is related to the Faraday effect [18,19]. Faraday rotation for composite media made of small particles embedded in the dielectric host was intensively studied, primarily by Stroud *et al.* [18–21]. The model predicts a linear response to the magnetic field and an anomalously large increase of the Faraday constant close to the nanoparticle surface plasmon frequency. The Stroud theory for ferrofluids has later been extended to anisotropic inclusions with the application to conducting polymers [22]. Increase of the Faraday rotation close to the surface plasmon frequency was experimentally confirmed for the magnetic Fe<sub>2</sub>O<sub>3</sub> nanoparticles dispersed in wax [23]. Here we present a study of magnetically induced optical activity in ferrofluids made of spherical cobalt (Co) nanoparticles of different sizes suspended in an organic solvent. Similar systems have been studied before; however, in this paper we show that the quantitative analysis of the Faraday rotation enables the determination of important parameters such as the magnetic moment of a single particle and the

surface plasmon frequency of the particle, which are difficult to obtain by other methods.

## II. THEORETICAL CONSIDERATIONS

### A. Dielectric tensor of the composite material

Optical properties of composite materials can be expressed by the effective dielectric tensor  $\underline{\varepsilon}_{\text{eff}}$ , which includes the information about the optical properties of the host and inclusion (nanoparticles):

$$\underline{\varepsilon}_{\text{eff}} = \begin{vmatrix} \varepsilon_1^{\text{eff}} & iA^{\text{eff}} & 0 \\ -iA^{\text{eff}} & \varepsilon_1^{\text{eff}} & 0 \\ 0 & 0 & \varepsilon_2^{\text{eff}} \end{vmatrix}.$$

The host is optically isotropic in zero external field. If the magnetic field is applied along the  $z$  axis, the dielectric tensor of the host ( $\underline{\varepsilon}_h$ ) becomes anisotropic and optically active and can be expressed as:

$$\underline{\varepsilon}_{\text{eff}} = \begin{vmatrix} \varepsilon_{h1} & iA_h & 0 \\ -iA_h & \varepsilon_{h1} & 0 \\ 0 & 0 & \varepsilon_{h2} \end{vmatrix}.$$

The dielectric tensor of the inclusion is also anisotropic, if particles are not spherical (shape anisotropy) or if they are magnetized having internal magnetic field already built-in. The dielectric tensor  $\underline{\varepsilon}_i$  in the eigenframe of the nanoparticle is, thus:

$$\underline{\varepsilon}_{\text{eff}} = \begin{vmatrix} \varepsilon_{i1} & iA_i & 0 \\ -iA_i & \varepsilon_{i1} & 0 \\ 0 & 0 & \varepsilon_{i2} \end{vmatrix}.$$

To express the dielectric tensor of the inclusion in the laboratory frame with the  $z$  axis along the direction of the external magnetic field, one has to take into account that the axes of the eigen coordinate system of the inclusion are rotated by the angles  $(\theta, \varphi)$  with respect to the dielectric tensor

\*jacek.szczytko@fuw.edu.pl

axes of the host  $\underline{\varepsilon}_i$ , so the dielectric tensor of the inclusion in the laboratory frame is  $\underline{\varepsilon}_i(\theta, \varphi) = \underline{R}\underline{\varepsilon}_i\underline{R}^T$ , where  $\underline{R}$  is the rotation matrix:

$$\underline{R}(\theta, \varphi) = \begin{pmatrix} \cos \varphi & \sin \varphi \cos \theta & \sin \varphi \sin \theta \\ -\sin \varphi & \cos \varphi \cos \theta & \cos \varphi \sin \theta \\ 0 & -\sin \theta & \cos \theta \end{pmatrix}.$$

The exact form of the effective dielectric tensor can be found knowing the dielectric tensors  $\underline{\varepsilon}_h$  and  $\underline{\varepsilon}_i$ . In the case of the host material, the anisotropy induced by the external magnetic field can be easily measured and taken into account in the later analysis of the experimental data. For the inclusions, the dependence of the dielectric tensor on the wavelength, particle shape, size, etc. must be found theoretically, since it is very difficult (or even impossible) to measure the dielectric tensor of a single nanoparticle.

We search for the effective medium tensor  $\underline{\varepsilon}_{\text{eff}}$  by assuming that the polarizability of the effective medium results from the polarizability of the inclusions in the host [24]. For a small concentration of nanoparticles (denoted by the volume fraction, also called the filling factor,  $f \ll 1$ ), one can neglect the interactions among nanoparticles, and for the spherical inclusions the effective dielectric tensor is expressed as [22,25,26]

$$\underline{\varepsilon}_{\text{eff}} \approx \underline{\varepsilon}_h + 3\varepsilon_h f \langle \underline{M} \rangle_R, \quad (1)$$

where

$$\underline{M} = [\underline{\varepsilon}_i(\theta, \varphi) + 2\underline{\varepsilon}_h]^{-1}[\underline{\varepsilon}_i(\theta, \varphi) - \underline{\varepsilon}_h]$$

and  $\langle \dots \rangle_R$  denotes the average over all the possible orientations of the inclusions. The components of the dielectric tensor of the metallic inclusions [Eq. (1)] are acquired from the Drude model, assuming weakly bounded electrons in a static magnetic field and the harmonic electric field of the incident light,

$$\begin{aligned} \varepsilon_{i1} &= 1 + \frac{i(1 - i\omega\tau)(\omega_p\tau)^2}{\omega\tau[(1 - i\omega\tau)^2 + (\omega_c\tau)^2]} \\ \varepsilon_{i2} &= 1 + \frac{i(\omega_p\tau)^2}{\omega\tau(1 - i\omega\tau)} \\ A_i &= \frac{(\omega_p\tau)^2\omega_c\tau}{\omega\tau[(1 - i\omega\tau)^2 + (\omega_c\tau)^2]}, \end{aligned}$$

where  $\omega_p$  is the plasma frequency  $\omega_p = Ne^2/(\varepsilon_0 m^*)$ ,  $m^*$  is the effective mass of the electron,  $e$  is its charge,  $N$  is the electron number density, and  $\tau$  is the characteristic lifetime of momentum relaxation. For the cyclotron frequency  $\omega_c$ , we assume the following dependence

$$\omega_c = e(B_m + B_{\text{ext}} \cos \theta)/m^*, \quad (2)$$

where  $B_m$  is the internal magnetic flux density due to the ferromagnetic magnetization,  $B_{\text{ext}}$  is the external magnetic flux density, and  $\theta$  is the angle between  $B_{\text{ext}}$  and the nanoparticle magnetic dipole  $\mu$  that is parallel to  $B_m$ . The vector sum of  $B_m$  and  $B_{\text{ext}}$  gives the total internal magnetic flux density in the nanoparticle. In the case of  $B_{\text{ext}}$  being lower than  $B_m$ , the magnitude of the internal magnetic flux density is approximately  $B_m + B_{\text{ext}} \cos \theta$ , which was used in the expression for the cyclotron frequency [Eq. (2)].

In order to underline the importance of the magnetic field on optical activity, we rewrite  $A_i$  in the form

$$A_i = A_{i0} \left( 1 + \frac{B_{\text{ext}}}{B_m} \cos \theta \right),$$

where

$$A_{i0} = \frac{(\omega_p\tau)^2\omega_c\tau}{\omega\tau[(1 - i\omega\tau)^2 + (\omega_c\tau)^2]}$$

and  $\omega_c = eB_m/m^*$ .

The external magnetic field aligns magnetic moments of ferromagnetic nanoparticles. In order to get the effective dielectric tensor, one should sum up the contributions of the nanoparticle dielectric tensors according to the thermodynamical distribution of nanoparticle magnetic moment orientations in the external magnetic field at finite temperature. Since the calculation of average required by Eq. (1) is rather comprehensive in a general case, we make a reasonable simplification and assume that the dielectric tensors of the host and the inclusion are not birefringent ( $\varepsilon_{h1} = \varepsilon_{h2} = \varepsilon_h$  and  $\varepsilon_{i1} = \varepsilon_{i2} = \varepsilon_i$ ). We calculate the orientational average of the matrix  $\underline{M}$  as

$$\langle \underline{M} \rangle_R = \frac{1}{Z} \frac{1}{4\pi} \int_0^1 d \cos \theta \int_0^{2\pi} d\varphi \underline{M} \exp\left(\frac{\mu B_{\text{ext}} \cos \theta}{k_B T}\right),$$

where  $Z = -\sinh x/x$  is the statistical sum with  $x = \mu B_{\text{ext}}/k_B T$ ,  $k_B$  is the Boltzmann constant,  $T$  is temperature, and  $\mu$  is the magnetic moment of a single nanoparticle. Performing the integration, one finds the following expressions for the nonzero matrix elements:

$$\begin{aligned} M_{11} &= M_{22} = M_{33} = \frac{\varepsilon_i - \varepsilon_h}{\varepsilon_i + 2\varepsilon_h} \\ M_{12} &= -M_{21} = \frac{3i A_{i0} \varepsilon_h}{(\varepsilon_i + 2\varepsilon_h)^2} \left\{ \frac{B_{\text{ext}}}{B_m} \left[ 1 - 2 \frac{L(x)}{x} \right] + L(x) \right\}, \end{aligned}$$

where  $L(x) = \coth x - 1/x$  is the Langevin function. Having the elements of the tensor  $\langle \underline{M} \rangle_R$ , the following elements of the effective dielectric tensor are obtained from Eq. (1):

$$\varepsilon_1^{\text{eff}} = \varepsilon_2^{\text{eff}} = \varepsilon_h \left( 1 + 3f \frac{\varepsilon_i - \varepsilon_h}{\varepsilon_i + 2\varepsilon_h} \right) \quad (3)$$

$$A^{\text{eff}} = A_h + 9f\varepsilon_h^2 \frac{A_{i0}}{(\varepsilon_i + 2\varepsilon_h)^2} \left\{ \frac{B_{\text{ext}}}{B_m} \left[ 1 - 2 \frac{L(x)}{x} \right] + L(x) \right\}, \quad (4)$$

where in the expression for  $A^{\text{eff}}$  we have neglected the term of the order  $f A_h$ . As expected, without the external magnetic field,  $A^{\text{eff}} = 0$  and the system is not optically active.

## B. Optical activity (Faraday effect)

In the Faraday configuration, the light propagates along the direction of the external magnetic field. Setting this direction as the  $z$  axis, the wave vector is  $\vec{k} = (0, 0, k)$  (where  $k = 2\pi/\lambda$ ), polarization of the incident light (with the wave vector  $\vec{k}_0$  and wavelength  $\lambda_0$ ) is in the  $xy$  plane [ $\vec{E} = (E_x, E_y, 0)$ ], and the external magnetic field is  $\vec{B}_{\text{ext}} = (0, 0, B)$ . By solving the wave equation for this configuration,

$$\vec{k} \times (\vec{k} \times \vec{E}) + k_0^2 \underline{\varepsilon}_{\text{eff}} \vec{E} = 0,$$

one obtains two circularly polarized eigenmodes,  $E_y = \pm i E_x$ , with the wave vectors

$$k_{\pm} = k_0 \sqrt{\varepsilon_1^{\text{eff}} \pm A^{\text{eff}}}.$$

The Faraday rotation angle per unit length is

$$\theta_F = \text{Re} \left[ \frac{1}{2} (k_+ - k_-) \right] = \text{Re} \left[ \frac{k_0 A^{\text{eff}}}{2 \sqrt{\varepsilon_1^{\text{eff}}}} \right], \quad (5)$$

where the fact that the off-diagonal terms are very small was used. Using Eqs. (3) and (4) in Eq. (5), assuming  $\varepsilon_1^{\text{eff}} \approx \varepsilon_h$  and subtracting the Faraday rotation due to the host, the Faraday rotation due to the inclusion of nanoparticles  $\theta_F^i$  can be expressed as

$$\theta_F^i = \frac{\omega c_0}{c} f K(\omega) \left\{ \frac{B_{\text{ext}}}{B_m} \left[ 1 - 2 \frac{L(x)}{x} \right] + L(x) \right\}, \quad (6)$$

where the function  $K(\omega)$ , dependent on material parameters of host and inclusions, is defined as

$$K(\omega) = \frac{1}{2} \frac{9}{1 + 2\varepsilon_h} \varepsilon_h^{3/2} (\omega_p^* \tau)^2 \frac{1 - \left(1 - \frac{\omega_p^{*2}}{\omega^2}\right)^2 \omega^2 \tau^2}{\left[1 + \left(1 - \frac{\omega_p^{*2}}{\omega^2}\right)^2 \omega^2 \tau^2\right]^2}, \quad (7)$$

with a surface plasmon frequency of spherical particle  $\omega_p^* = \omega_p / \sqrt{1 + 2\varepsilon_h}$  [27,28].

The properties of the host (pure solvent) are known, as they can be easily found in literature or measured. The linear dependence of the elements of the effective dielectric tensor on the properties of the host tensor allows the subtraction of the results obtained for the pure host material from results obtained for the composite material. The relaxation time  $\tau$  can be treated as a fitting parameter; however, in order to restrict the number of free parameters in the model, one can estimate it from the nanoparticle diameter  $d$  and the value of the carrier velocity ( $v_F$ ) at the Fermi energy (about  $1.0 \times 10^6$  m/s [29]), so  $\tau \sim d/v_F$  is of the order of  $2 \times 10^{-14}$  s. The effective mass  $m^*$  is assumed to be equal to the electron mass. The internal magnetic flux density  $B_m$  was estimated [30] from the bulk magnetization ( $M$ ) of cobalt as  $B_m = \mu_0(M - LM)$ , where  $L = 1/3$  is the depolarization factor for spherical geometry. We calculate magnetization as  $M = \mu_1 \rho N_A / M_{Co}$ , where  $\mu_1 = 1.751 \mu_B$  is the magnetic moment of a single cobalt atom in number of Bohr magnetons  $\mu_B$ ,  $\rho = 8.9 \text{ g/cm}^3$  is the density of cobalt,  $M_{Co} = 59 \text{ g/mol}$  is its molar mass, and  $N_A$  is the Avogadro number. We find  $B_m = 1.23 \text{ T}$ . The magnetic moment  $\mu$  of a single nanoparticle is considered as a fitting parameter, since due to the surface effects the magnetic moment of a nanoparticle is expected to be lower than the sum of magnetic moments of Co atoms in the nanoparticle [31,32]. The plasma frequency is also taken as a fitting parameter, since in the nanosized material it can differ from the bulk value. The volume fraction  $f$  of the nanoparticles and the particle diameter  $d$  were measured as described in the next section. However, the measurements of the volume fraction are unreliable due to the rather fast evaporation of the solvent. Because of that we decided to take the volume fraction as a fitting parameter as well. Therefore, finally, we have a set of three fitting parameters:  $\omega_p$ ,  $\mu$ , and  $f$ .

### III. EXPERIMENTAL SETUP AND MEASUREMENTS

The Co nanoparticles were synthesized by the high-temperature decomposition of an organometallic precursor—octacarbonyldicobalt,  $\text{Co}_2(\text{CO})_8$ , in the o-dichlorobenzene solution under inert (Ar) atmosphere, in the presence of organic surfactants: trioctylphosphane oxide (TOPO) and oleic acid (OA), to prevent particles aggregation. After the reaction, the Co particles were precipitated by the addition of anhydrous acetone and redissolved in a nonpolar solvent such as cyclohexane. The obtained particles were spherical, their diameter could be controlled by the TOPO/OA ratio used in the synthesis. The metal core diameter was estimated by the small angle x-ray scattering (SAXS), from particles dissolved in cyclohexane. The BrukerNanoStar x-ray system and NanoFit software was used. The size of nanoparticles was also checked by the transmission electron microscopy (TEM). Nanoparticles with the metal core diameters from 3 to 11 nm were studied. The size distribution was less than 10%.

For the magneto-optical measurements, mixtures with different concentrations of nanoparticles in cyclohexene were prepared. The concentration of nanoparticles was determined assuming that UV absorption increases linearly with particle concentration.

The setup for Faraday rotation measurements consisted of a light source (He-Ne laser of 5 lines with  $\lambda = 543 \text{ nm}$ ,  $594 \text{ nm}$ ,  $604 \text{ nm}$ ,  $612 \text{ nm}$ , and  $633 \text{ nm}$ ), optical chopper with a defined frequency to modulate the beam (in order to measure total light intensity  $I_{\text{Tot}}$  with lock-in amplifier), and a set of filters to reduce the intensity of light at the detector (if needed). The light propagated through the first polarizer  $P1$  and then through the sample placed in the induction coil, generating homogenous magnetic field up to 0.4 T. The light transmitted through the sample was modulated by the photoelastic modulator (PEM, working at a basic frequency  $\Omega = 50 \text{ kHz}$  and maximal retardation  $\lambda/4$ ). Finally, the light passed through the linear polarizer  $P2$ . The polarizer  $P1$  was parallel to the PEM axis and  $P2$  was at 45 degrees to it. Transmitted light was detected by the silicon diode and the output signal was analyzed by the lock-in amplifier.

Quantitative information about optical properties of a sample is given by the ratio of the signal intensities at  $\Omega$  ( $I_{\Omega}$ ) and  $2\Omega$  (second-harmonic,  $I_{2\Omega}$ ). Optically active sample is characterized by the second harmonic signal at frequency  $2\Omega$ . The Faraday rotation angle  $\theta_F$  is determined as:

$$\theta_F = \arcsin \left[ -\frac{I_{2\Omega}}{4J_2\left(\frac{\pi}{2}\right) T_f T_s} \right],$$

where  $J_n(\frac{\pi}{2})$  is the  $n$ th Bessel function of the first kind and

$$T_f = \sqrt{\frac{1}{2} \left[ I_{\text{Tot}} + \frac{1}{2} I_{2\Omega} \frac{J_0\left(\frac{\pi}{2}\right)}{J_2\left(\frac{\pi}{2}\right)} - I_{\Omega} \frac{1}{2J_1\left(\frac{\pi}{2}\right)} \right]}$$

$$T_s = \sqrt{\frac{1}{2} \left[ I_{\text{Tot}} + \frac{1}{2} I_{2\Omega} \frac{J_0\left(\frac{\pi}{2}\right)}{J_2\left(\frac{\pi}{2}\right)} + I_{\Omega} \frac{1}{2J_1\left(\frac{\pi}{2}\right)} \right]}$$

are the fast ( $T_f$ ) and slow ( $T_s$ ) transmission coefficients for circularly polarized light, i.e., eigen polarization modes of the system. The lock-in detection enables the high-sensitivity

measurements of optical activity; rotations as small as  $10^{-2}$  degree/cm can be measured. According to Eq. (4) the obtained results were corrected by the Faraday rotation of a pure host (i.e., cyclohexane in all cases).

#### IV. RESULTS AND DISCUSSION

##### A. Plasma frequency

The plasma frequency was obtained from the measurements of the Faraday rotation for nanoparticles with  $d = 11.0$  nm (measured by SAXS) at five different wavelengths (Fig. 1). The fitting of the plasma frequency was performed at the saturated value of the Faraday rotation angle (Fig. 2) at  $B_{\text{ext}} = 0.4$  T. The steepness of the curve in Fig. 2 is defined by parameter  $K(\omega)$  [Eq. (7)], and it is very sensitive to the value of the plasma frequency. The fit to the absolute value of the saturated angle is obtained by fitting the product  $f\{\frac{B_{\text{ext}}}{B_m}[1 - 2\frac{L(x)}{x}] + L(x)\}$  [see Eq. (6)] after the plasma frequency is found. The best fit was obtained for the plasma frequency corresponding to the wavelength  $\lambda_p = (198 \pm 7)$  nm, which corresponds to  $(6.3 \pm 0.2)$  eV. The value of the plasma frequency is not significantly sensitive to the changes in the relaxation time  $\tau$ . We fitted it at  $\tau = 2 \times 10^{-14}$  s; however, we have obtained the same fit for the plasma frequency at the relaxation times greater than  $8 \times 10^{-15}$  s. Since we are in the region of saturation [ $L(x) \approx 1$  and  $L(x)/x \approx 0$ ], we find that  $\{\frac{B_{\text{ext}}}{B_m}[1 - 2\frac{L(x)}{x}] + L(x)\} \approx 1.3$ ; thus, the fitted value of volume fraction is  $f \approx 9 \times 10^{-5}$ . The volume fraction of the Co-nanoparticles was estimated by absorption measurements to be  $f \approx 5 \times 10^{-5}$ . So the values are in reasonable agreement.

The fitted value of the plasma frequency is in a reasonable agreement with the values of  $\omega_p$  presented in literature for bulk materials ranging from 318 nm (3.9 eV) [33] to 162 nm (7.66 eV) [34]. However, we note that the values in literature are usually reported for the fcc Co, while nanoparticles usually

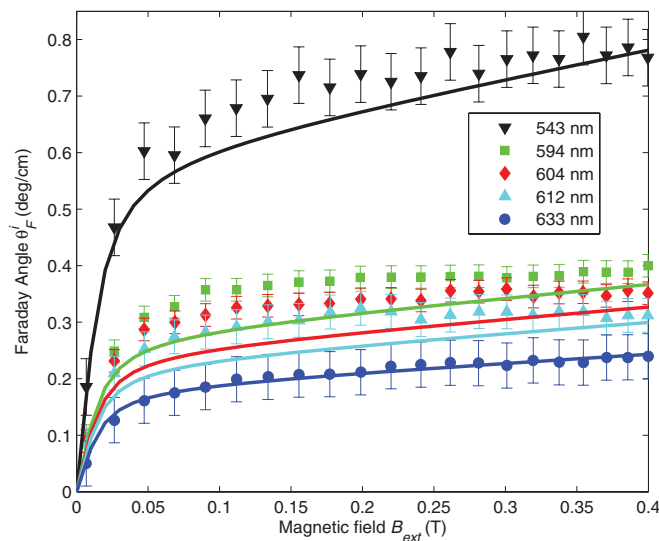


FIG. 1. (Color online) Faraday rotation angle due to the inclusion of nanoparticles ( $\theta_F^i$ ) vs. external magnetic field ( $B_{\text{ext}}$ ) at different wavelengths of light. Experimental data are marked as points, theoretical curves are solid lines.

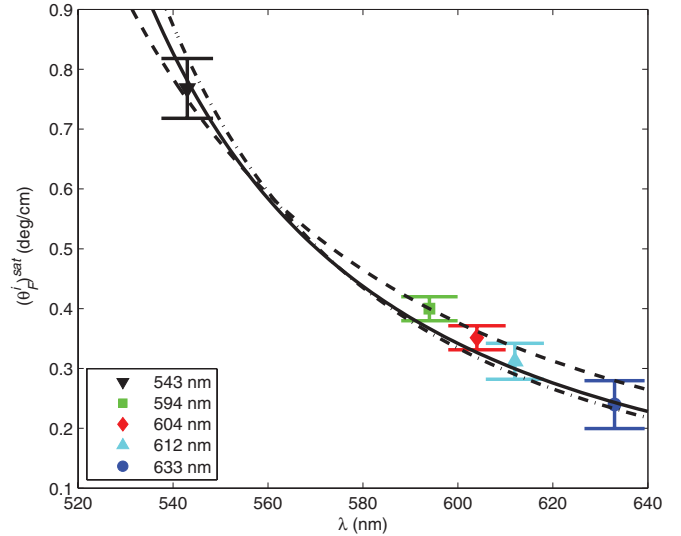


FIG. 2. (Color online) Saturated value of Faraday rotation angle  $(\theta_F^i)^{\text{sat}}$  vs. wavelength of light  $\lambda$ . Solid line represents fit with  $\omega_p = 198$  nm,  $f = 9.2 \times 10^{-5}$ , dashed lines is for 188 nm ( $f = 1.4 \times 10^{-4}$ ) and dot-dashed line is for 202 nm ( $f = 7.8 \times 10^{-5}$ ). Experimental data are marked as points.

crystallize in  $\epsilon$ -Co structure [34], which can, to some extent, influence the value of  $\omega_p$ .

##### B. Magnetic moment of a single nanoparticle

Knowing the plasma frequency  $\omega_p$ , one can find the magnetic moment  $\mu$  of a single nanoparticle by fitting  $\theta_F^i$  [Eq. (6)], which is a function of  $x = \mu B_{\text{ext}}/k_B T$  to the Faraday rotation angle versus external field  $B_{\text{ext}}$ . For nanoparticles with  $d = 11.0$  nm, we find  $\mu = 60 \times 10^3 \mu_B$ . Since the plasma frequency does not depend significantly on the relaxation time, one can assume that for the particles with  $d = 3.6$  and  $6.3$  nm (determined also by SAXS) it is the same as for the 11-nm particles. Then we can fit also the magnetic moments for the 3.6- and 6.3-nm particles and find  $\mu = 9.8 \times 10^3 \mu_B$  and  $\mu = 3.5 \times 10^3 \mu_B$ , respectively (Fig. 3).

From the nanoparticle magnetic moment one can calculate the magnetic moment of a single atom or estimate the effective magnetic diameter and the thickness of the nonmagnetic shell as discussed below.

##### C. Effective magnetic diameter and thickness of the nonmagnetic shell

If we want to estimate the size of the effective magnetic diameter of a single nanoparticle, we write the magnetic moment of a nanoparticle as

$$\mu = \mu_1 N(d_m),$$

where  $N(d_m)$  is the number of atoms with the magnetic moment  $\mu_1 = 1.751 \mu_B$  equal to the bulk value for Co [35,36]. We find the effective magnetic diameter  $d_m$  such that the magnetic moment equals the experimentally obtained value. The obtained value presents the diameter of the magnetic core of the nanoparticle inside which the atoms in the nanoparticle behave as in the bulk, while on the surface they

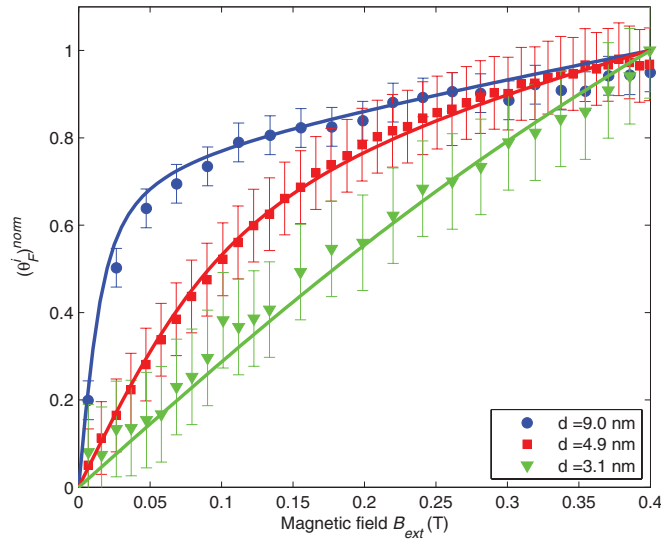


FIG. 3. (Color online) The normalized Faraday rotation angle  $(\theta_F^i)^{\text{norm}}$  vs. magnetic field ( $B_{\text{ext}}$ ) for three solutions of particles with different diameters of the magnetic core. The diameter was calculated assuming the bulk value of the magnetic moment of an atom ( $1.751 \mu_B$ ). The experiment was performed with the He-Ne laser 633 nm line.

are treated as nonmagnetic [31,32]. This provides the insight into the magnetic properties of nanoferrromagnets. We obtain the effective magnetic diameters equal to 3.1, 4.9, and 9.0 nm for the particles for which the SAXS measurements give 3.6, 6.3, and 11 nm, respectively. The nonmagnetic Co shell around the magnetic core is formed because the spin-exchange interaction of the atoms at the surface of nanoparticle is weaker than inside, because of the lack of neighbors and rearrangement of chemical bonds [37]. We see that the nonmagnetic shell of the nanoparticle is 0.5 to 1.0 nm thick, which amounts to the thickness of 2 to 4 Co atom diameters.

## V. CONCLUSIONS

The Faraday rotation in the mixtures of Co-nanoparticle inclusions in the cyclohexene host was studied experimentally and theoretically. By calculating the effective dielectric

tensor, taking into account the orientational distribution of nanoparticle magnetic moments in external magnetic field we were able to find the value of the plasma frequency in the Co nanoparticles, their effective magnetic diameter, and the average value of the magnetic moment of one nanoparticle.

The obtained plasma frequency corresponding to the wavelength  $\lambda_p = (198 \pm 7)$  nm is close to the bulk value, showing that the free electron concentration in metal is only weakly affected by the size of the nanoparticle.

The procedure presented in this paper enables estimation of the magnetic moment of a single nanoparticle, which is hard to obtain by other methods. From the magnetic moment of a nanoparticle one can find the magnetic moment of a single atom if the size of the particle is known from some other experimental method. By assuming the bulk value of the atom magnetic moment, one can estimate the effective magnetic diameter of nanoparticles. We find that the nonmagnetic shell of the nanoparticle is 0.5 to 1.0 nm thick, which amounts to the thickness of few Co atoms (2 to 4).

Knowing the effective magnetic diameter and comparing with the real diameter obtained from electron microscopy, one can model important internal properties of magnetic nanoparticle like internal stress, anisotropy, surface versus bulk properties, etc. Therefore, the presented experimental method of measuring the effective magnetic diameter of nanoparticles suspended in a solution provides a tool for both experimental and theoretical (numerical, see, e.g., Ref. [38]) investigations of ferromagnetic nanoparticles of different metals and in principle can give insight into internal properties of nanoferrromagnets.

## ACKNOWLEDGMENTS

The authors thank Dr. Marko Jagodič for fruitful discussions on the magnetic properties of ferromagnetic nanoparticles. The authors acknowledge the TEAM program from FNP (Project No. TEAM/2010-5/4, self-assembly of functionalized inorganic-organic liquid crystalline hybrids for multifunctional nanomaterials) for financial support. This work was also supported by the Slovenian-Polish joint research project liquid crystalline phases made by metal nanoparticles and the Slovenian ARRS research program P1-0055.

- 
- [1] W. Luo, T. Du, and J. Huang, *Phys. Rev. Lett.* **82**, 4134 (1999).
  - [2] J. W. Seo, S. J. Park, and K. O. Jang, *J. Appl. Phys.* **85**, 5956 (1999).
  - [3] Yu. N. Skibin, V. V. Chekanov, and Yu. L. Raizer, *Zh. Eksp. Teor. Fiz.* **72**, 949 (1977) [*Sov. Phys. JETP* **45**, 496 (1977)].
  - [4] P. C. Scholten, *IEEE Trans. Magn.* **16**, 221 (1980).
  - [5] S. Taketomi, *Jpn. J. Appl. Phys., Part 1* **22**, 1137 (1983).
  - [6] E. Hasmonay, E. Dubois, J.-C. Bacri, R. Perzynski, Yu. L. Raikher, and V. I. Stepanov, *Eur. Phys. J. B* **5**, 859 (1998).
  - [7] M. Rasa, *J. Magn. Magn. Mater.* **201**, 170 (1999).
  - [8] A. F. Pshenichnikov and V. M. Buzhakov, *Colloid J.* **63**, 305 (2001).
  - [9] E. Hasmonay *et al.*, *J. Appl. Phys.* **88**, 6628 (2000).
  - [10] A. Martinet, *Rheol. Acta* **13**, 260 (1974).
  - [11] J. P. Llewellyn, *J. Phys. D* **16**, 95 (1983).
  - [12] Q. Zhang and J. Wang, *J. Appl. Phys.* **78**, 3999 (1995).
  - [13] M. A. Osipov, P. I. C. Teixeira, and M. M. Telo da Gama, *Phys. Rev. E* **54**, 2597 (1996).
  - [14] James E. Martin, Kimberly M. Hill, and Chris P. Tigges, *Phys. Rev. E* **59**, 5676 (1999).
  - [15] B. R. Jennings, M. Xu, and P. J. Ridler, *J. Phys. D* **34**, 1617 (2001).
  - [16] Alexey O. Ivanov and Sofia S. Kantorovich, *Phys. Rev. E* **70**, 021401 (2004).
  - [17] Z. Di, X. Chen, S. Pu, X. Hu, and Y. Xia, *Appl. Phys. Lett.* **89**, 211106 (2006).

- [18] P. M. Hui and D. Stroud, *Appl. Phys. Lett.* **50**, 950 (1987).
- [19] T. K. Xia, P. M. Hui, and D. Stroud, *J. Appl. Phys.* **67**, 2736 (1990).
- [20] H. W. Davies and J. P. Llewellyn, *J. Phys. D: Appl. Phys.* **13**, 2327 (1980).
- [21] D. Stroud, *J. Appl. Phys.* **66**, 2585 (1989).
- [22] O. Levy and D. Stroud, *Phys. Rev. B* **56**, 8035 (1997).
- [23] N. A. Yusuf, A. A. Rousan, and H. M. El-Ghanem, *J. Appl. Phys.* **84**, 2781 (1988).
- [24] D. Stroud and F. P. Pan, *Phys. Rev. B* **13**, 1434 (1976); D. Stroud, *ibid.* **12**, 3368 (1975).
- [25] H. Ammari, H. Kang, and K. Kim, *J. Diff. Equat.* **215**, 402 (2005).
- [26] H. Kang and K. Kim, *J. Comp. Math.* **25**, 157 (2007).
- [27] Uwe Kreibitz and Peter Zacharias, *Z. Physik* **231**, 128 (1970).
- [28] D. J. Bergman and D. Stroud, in *Solid State Physics: Advances in Research and Applications*, Vol. 46 (Academic Press, San Diego, 1992), pp. 127–269.
- [29] M. Richter and H. Eschrig, *Solid State Commun.* **72**, 263 (1989).
- [30] J. M. D. Coey, *Magnetism and Magnetic Materials* (Cambridge University Press, Cambridge, 2009).
- [31] Y. Labaye, O. Crisan, L. Berger, J. M. Greneche, and J. M. D. Coey, *J. Appl. Phys.* **91**, 8715 (2002).
- [32] E. De Biasi, C. A. Ramos, R. D. Zysler, and H. Romero, *Phys. Rev. B* **65**, 144416 (2002).
- [33] M. E. Thomas, *Optical Propagation in Linear Media: Atmospheric Gases and Particles, Solid State Components, and Water* (Oxford University Press, New York, 2006).
- [34] E. D. Palik (ed.), *Handbook of Optical Constants of Solids II* (Academic Press, San Diego, 1991).
- [35] J. P. Chen, C. M. Sorensen, K. J. Klabunde, and G. C. Hadjipanayis, *Phys. Rev. B* **51**, 11527 (1995).
- [36] Landolt-Bornstein Database, Magnetic properties of 3d, 4d, and 5d elements, alloys and compounds—Spontaneous magnetization, magnetic moments, and high-field susceptibility, Springer Materials Database, p. 34.
- [37] H. Kachkachi and E. Bonet, *Phys. Rev. B* **73**, 224402 (2006); D. A. Garanin and H. Kachkachi, *Phys. Rev. Lett.* **90**, 065504 (2003).
- [38] H. Fangohr *et al.*, Nmag, computational magnetism (2012), <http://nmag.soton.ac.uk/nmag/>.